The American Journal of Pathology, Vol. 179, No. 2, August 2011

DOI: 10.1016/j.ajpath.2011.04.013

Neurobiology

Toll-Like Receptor 4 Promotes α-Synuclein Clearance and Survival of Nigral Dopaminergic Neurons

Nadia Stefanova,* Lisa Fellner,* Markus Reindl,* Eliezer Masliah,† Werner Poewe,* and Gregor K. Wenning*

From the Division of Clinical Neurobiology, Department of Neurology, Innsbruck Medical University, Innsbruck, Austria; and the Department of Neurosciences,† University of California, San Diego, School of Medicine, La Jolla, California*

Toll-like receptors (TLRs) mediate innate immunity, and their dysregulation may play a role in α-synucleinopathies, such as Parkinson's disease or multiple system atrophy (MSA). The aim of this study was to define the role of TLR4 in α-synuclein–linked neurodegeneration. Ablation of TLR4 in a transgenic mouse model of MSA with oligodendroglial α-synuclein overexpression augmented motor disability and enhanced loss of nigrostriatal dopaminergic neurons. These changes were associated with increased brain levels of α-synuclein linked to disturbed TLR4-mediated microglial phagocytosis of α-synuclein. Furthermore, tumor necrosis factor-α levels were increased in the midbrain and associated with a proinflammatory astroglial response. Our data suggest that TLR4 ablation impairs the phagocytic response of microglia to α-synuclein and enhances neurodegeneration in a transgenic MSA mouse model. The study supports TLR4 signaling as innate neuroprotective mechanism acting through clearance of α-synuclein. ***(Am J Pathol 2011, 179:954–963; DOI: 10.1016/j.ajpath.2011.04.013)***

α-Synuclein (AS) cytoplasmic inclusions are the pathological hallmark of Parkinson's disease (PD), dementia with Lewy bodies (DLB), and multiple system atrophy (MSA) commonly called α-synucleinopathies (ASPs). It is currently accepted that AS plays a major role in the pathogenesis of these disorders as suggested by genetic[1–3] and experimental studies on the toxicity of AS species.[4–14] Recent observations showed up-regulation of Toll-like receptors (TLRs) in ASPs,[15,16] but their contribution to the pathogenesis has not been studied. TLRs are a family of highly conserved molecules that recognize pathogen-associated molecular patterns, including both exogenous and endogenous ligands, and define the innate immunity response.[17] In the central nervous system different types of TLRs have been identified up-regulated in response to systemic or local insults.[18] TLR4 is associated with CD14-mediated lipopolysaccharide-induced inflammatory signaling, and several observations suggest its role in ischemic brain damage.[19,20] TLR2 and TLR4/CD14 complex have been associated with the removal of amyloid-β, indicating innate immunity receptors on microglia as a natural defense mechanism to prevent amyloid-β accumulation.[21–24]

Several models of both neuronal[25] and oligodendroglial[26] ASPs have been developed using targeted overexpression of AS. The proteolipid protein (PLP) human AS (hAS) mouse model represents a model of MSA-like neuropathology with oligodendroglial AS aggregates[27] associated with progressive microglial activation and nigral degeneration.[15] This model provides a suitable test bed to address questions related to AS-induced neuroinflammatory responses and neurodegeneration.

The main objective of the current study was to determine the role of TLR4 ablation on motor disability and neuronal loss in the PLP transgenic mouse model of ASPs. We used behavioral, morphologic, biochemical, and cell culture assays to analyze the effect of TLR4 deficiency. TLR4 deficiency was associated with suppression of microglial AS phagocytosis, resulting in poor AS clearance and accelerated neurodegeneration in the ASP model.

Materials and Methods

Transgenic Mouse Lines

Homozygous AS transgenic mice harboring the hAS under the control of the PLP promoter[27] were cross-bred with TLR4$^{-/-}$ mouse strain (C57BL/10ScNJ with a deletion of the *TLR4* gene), so that they fail to express TLR4 mRNA and protein,[28] to get first-generation heterozygous

Supported by grants of the Austrian Science Funds P19989-B05 and SFB F44-B19 and National Institutes of Health grants NS044233, AG5131, AG18440, AG022074, and NS057096.

Accepted for publication April 14, 2011.

Address reprint requests to Nadia Stefanova, M.D., Ph.D., Division of Clinical Neurobiology, Department of Neurology, Anichstr. 35, 6020 Innsbruck, Austria. E-mail: nadia.stefanova@i-med.ac.at.

Table 1. Primer Pairs and Product Sizes Used for Genotyping

Gene	Product size, bp	Primer pair
Human AS	450	Forward: 5′-ATGGATGTATTCATGAAAGG-3′ Reverse: 5′-TTAGGCTTCAGGTTCGTAG-3′
Mouse *CX32*	831	Forward: 5′-GACAGGGTCTCATTATGTAGCCTTA-3′ Reverse: 5′-CTGCGATGCTACAGTATCTCAAGTA-3′
Mouse *TLR4*	415	Forward: 5′-GAGATGAATACCTCCTTAGTGTTGG-3′ Reverse: 5′-ATTCAAAGATACACCAACGGCTCTGA-3′
Mouse *AS*	760	Forward: 5′-CTCAGGGTCGACTGCCTTAG-3′ Reverse: 5′-TGCACTCGAAGAGTCCCTTT-3′

CX32, connexin 32; Fwd, forward; Rev, reverse.

mice for both genes ($AS^{+/-}$, $TLR4^{+/-}$). First-generation double-heterozygous mice were further bred to generate in the second-generation AS-expressing TLR4-deficient mice (either $AS^{+/+}$,$TLR4^{-/-}$ or $AS^{+/-}$,$TLR4^{-/-}$). To select for the double-homozygous line, AS-expressing TLR4-deficient mice were bred for at least three further generations, and only families with 100% AS-expressing TLR4-deficient offspring were kept. All mice were genotyped by tail clip using two subsequent PCR reactions for hAS (controlled versus mouse connexin 32) and mouse TLR4 (controlled versus mouse AS) using the primers indicated in Table 1. The generation of the PLP-AS mouse was previously described.[27] Homozygous PLP-AS transgenic mice were initially provided by Philipp Kahle, Munich, Germany, and further bred at the Animal Facility of Innsbruck Medical University. Homozygous C57BL/10ScNJ mice[28] were purchased at Jackson Laboratories (stock No. 003752) and further bred at the Animal Facility of Innsbruck Medical University. All experiments were performed according to the Austrian law and with permission by the Federal Ministry for Science and Research of Austria. Animals were housed under a 12-hour light/dark cycle with food and water available *ad libitum*. All efforts were made to minimize the number of animals used and their suffering.

Phenotypic characterization of mice overexpressing hAS with normal TLR4 expression (assigned here as AS,$TLR4^{+/+}$) and mice with overexpression of hAS and TLR4 deficiency (assigned here as AS,$TLR4^{-/-}$) was performed at 6 months of age. To collect brain tissue, mice were deeply anesthetized via an i.p. injection of thiopental and then perfused intracardially with PBS followed by ice-cold 4% paraformaldehyde in PBS, pH 7.4. Brains were rapidly removed from skulls, postfixed overnight in the same fixative at 4°C, and cryoprotected in 25% sucrose in PBS. Frozen brains were cut serially (40-μm-thick sections) using a cryostat (Leica, Nussloch, Germany).

For protein analysis, mice were anesthetized with thiopental and perfused intracardially with PBS to remove blood from organs, brains were quickly removed, and blocks of forebrain and midbrain were dissected, snap frozen in liquid nitrogen, and finally stored at −80°C. Probes were homogenized on ice in lysis buffer containing Complete Mini Protease Inhibitor Cocktail (Roche Applied Science, Indianapolis, IN), protein concentration was measured by bicinchoninic acid protein assay (Sigma-Aldrich, St. Louis, MO), and aliquots for further analysis were stored at −80°C.

Behavioral Analyses

The behavioral experimenter was masked to the genetic status of the animals. To test locomotor disability, mice were tested in a pole test and an open field test. In the first paradigm we evaluated the ability of each mouse to climb down a vertical wooden pole with a rough surface, 1 cm wide and 50 cm high, as a measure of bradykinesia, balance, and coordination. Each mouse was placed with the head up at the top of the pole, and the time for turning downwards and the total time for climbing down the pole until the mouse reached the floor with the four paws were taken in five trials. The best performance of each mouse was kept for the statistical analysis.[29,30] In the second paradigm, spontaneous locomotor activity within a 15-minute interval in an open field arena was measured by Flex Field Activity System (San Diego Instruments, San Diego, CA), which allows monitoring and real-time counting of horizontal and vertical locomotor activity by 544 photo-beam channels. Mice were placed in the center of the open field (40.5 × 40.5 × 36.5 cm) and tested always at the same time of the day (6 PM). The tests were performed in a dark room that is completely isolated from external noises and light during the test period.[30]

Neuropathology, Confocal Microscopy, and Stereologic Analysis

The following primary antibodies were used in this study: monoclonal mouse antidopamine and cyclic AMP–regulated phosphoprotein (DARPP-32; a generous gift of Prof. Hugh Hemmings, New York, NY), monoclonal mouse antityrosine hydroxylase (TH; Sigma), monoclonal rat anti-hAS (15G7; a generous gift of Prof. Philipp Kahle, Tübingen, Germany), monoclonal rat anti-mouse CD11b (Serotec, Oxford, England), monoclonal mouse anti–glial fibrillary acidic protein (GFAP; Millipore, Temecula, CA), and purified anti-mouse tumor necrosis factor (TNF)-α (BioLegend, San Diego, CA). Immunohistochemistry (IHC) was performed according to standard protocols. Shortly, free-floating sections were treated with 0.3% H_2O_2 to quench endogenous peroxidase activity, then permeabilized or blocked in solution containing 0.1% Triton X-100, 1% bovine serum albumin, and 10% normal serum (from goat or horse as appropriate) in PBS. Sections were thereafter incubated with primary antibody overnight at 4°C, then incubated with the appropriate secondary antibody (bio-

tinylated anti-mouse IgG or anti-rat IgG; Vector Laboratories, Burlingame, CA), followed by Elite ABC complex (Vector Laboratories), and the reaction was visualized by 3,3′-diaminobenzidine. For immunofluorescence, Alexa 488– or Alexa 594–conjugated anti-rat or anti-mouse IgG (Jackson Immunoresearch Laboratories/Dianova, Hamburg, Germany) was applied.

Three-dimensional stacks were acquired with an SP5 confocal microscope (Leica Microsystems, Wetzlar, Germany) using a HCX PL APO 63x, 1.3 NA glycerol immersion objective. Imaging was performed using excitation with the 488-nm laser line for Alexa 488 and a 561-nm laser line for Alexa 594. Fluorescence emission was detected from 492 to 519 nm (Alexa 488) and from 594 to 742 nm (Alexa 594). Images were acquired using the Leica AF acquisition software version 2.2.1 (Leica Microsystems). The stacks were recorded according to the Nyquist criteria to allow deconvolution. Pixel sizes were therefore chosen as follows: x = 43.8 nm, y = 43.8 nm, and z = 125.9 nm. Image deconvolution was performed using Huygens Professional software version 3.6.0p2 (Scientific Volume Imaging, Hilversum, the Netherlands) to improve the resolution. For the SP5 images, a theoretical point spread function was then used to deconvolve the data using the Classical Maximum Likelihood Estimation Algorithm option of the software. Three-dimensional analysis was performed using Imaris x64 software version 7.1.0 (Bitplane, Zurich, Switzerland). Briefly, an isosurface was rendered onto the Alexa 594–positive cells to define the inner and outer borders of microglia, whereas spot detection was used to identify hAS-positive profiles. We then applied a clipping plane through the cell body and rotated it to view the cellular interior and thus identified the structures of interest.

Unbiased stereologic analysis was performed as previously described.[31] The number of dopaminergic neurons in substantia nigra pars compacta (SNc) and GABAergic medium spiny neurons in striatum was estimated by optical fractionator (Nikon E-800 microscope, Nikon digital camera DXM 1200; Stereo Investigator Software, MicroBrightField Europe e.K., Magdeburg, Germany). The density of striatal dopaminergic fibers was determined as previously described.[32] Briefly, serial sections throughout the striatum were captured at constant camera settings with the above mentioned equipment. TH staining brightness was measured in striatum ($OD_{striatum}$) and corpus callosum ($OD_{background}$) and the density of the striatal dopaminergic fibers (OD_{TH}) was calculated according to the following formula: $OD_{TH} = -\log (OD_{striatum}/OD_{background})$.

Electron Microscopy

Briefly, as previously described,[33] fixed brains were vibratomed at 40 μm and sections from transgenic AS,TLR4$^{+/+}$ and AS,TLR4$^{-/-}$ age-matched mice were postfixed in 1% glutaraldehyde, treated with osmium tetroxide, embedded in epon araldite, and sectioned with an ultramicrotome (Leica). Grids were analyzed with a Zeiss OM 10 electron microscope as previously described.[34] For immunogold labeling, sections were mounted in nickel grids, etched, and incubated with a rabbit polyclonal antibody against AS (Millipore, Temecula, CA) followed by labeling with a secondary antibody tagged with 10-nm Aurion ImmunoGold particles (1:50; Electron Microscopy Sciences, Fort Washington, PA) with silver enhancement. A total of 125 microglial cells were analyzed per condition. Cells were randomly acquired from three grids, and electron micrographs were obtained at magnifications of ×5000 and ×25,000.

Measurement of hAS Concentration by ELISA

Protein extracts from the midbrain and forebrain and supernatants from wild-type or PLP-AS mouse mixed glial culture were used to measure the level of hAS protein with an enzyme-linked immunosorbent assay (ELISA) kit (Invitrogen, Camarillo, CA) according to the protocol of the manufacturer.

Measurement of Cytokine Levels by Fluorometric Multiplex Bead–Based Immunoassay

FlowCytomix analysis, including application of the simplex kits for mouse TNF-α, mouse IL-6, mouse interferon (IFN)-γ, mouse granulocyte-macrophage colony-stimulating factor (GM-CSF), mouse IL-10, and mouse IL-1α, as well as the mouse basic kit (all from BenderSystems, Vienna, Austria), was performed according to the manufacturer protocol using protein extracts from the midbrain and forebrain.

Cell Culture

Three experimental approaches were used to define AS phagocytosis by microglial cells: (1) BV2 microglial cell line incubated with AS debris, (2) BV2 microglial cell line incubated with recombinant AS, and (3) primary microglia incubated with recombinant AS.

To demonstrate phagocytosis of AS-containing debris by BV2 microglia *in vitro,* we used previously described U373 cells overexpressing hAS.[10,14,35] AS-containing cells were brought into cell suspension of 2×10^6 cells/mL in Dulbecco's modified Eagle's medium (DMEM) and then underwent three consecutive freeze-thaw cycles of 30 minutes at −80°C followed by 15 minutes at +66°C. With this procedure, we achieved 100% cell death as controlled by classical Trypan blue staining. This AS debris suspension was kept at −80°C for further phagocytosis experiments. BV2 immortalized microglial cell line[36,37] (provided by Prof. Hubert Kerschbaum, Department of Animal Physiology, University of Salzburg, Salzburg, Germany) was seeded at a density of 9×10^5 per well in a 24-well plate with 1 mL of DMEM supplemented with 10% fetal calf serum (FCS). A total of 100 μL of the AS debris suspension was added to the BV2 cells, and after 5 minutes, 2 hours, and 24 hours image analysis was performed using a DMI4000B Leica microscope provided with Leica application software and Digital FireWire Color Camera DFC300 FX (Leica Microsystems).

To confirm AS phagocytosis by BV2 microglia and define the role of TLR4, BV2 cell cultures were exposed to 3 μmol/L recombinant AS with or without functional blocking of TLR4 achieved by 30-minute pretreatment of the

cells with anti-mouse TLR4/MD2 antibody clone MTS510 (BioLegend, San Diego, CA). Recombinant wild-type hAS protein was prepared as follows. Full-length hAS was amplified from human spinal cord cDNA (Clontech, Palo Alto, CA) by PCR as previously described.[14] The complete AS coding sequence was cloned into the prokaryotic expression vector pET101/D-TOPO (Invitrogen, Lofer, Austria) according to the manufacturer's instructions. After sequence analysis, protein expression was induced using isopropyl-β-thiogalactopyranoside (Sigma-Aldrich). The protein was purified by affinity chromatography applying nickel nitrilo-triacetic acid agarose (Qiagen, Hilden, Germany) and dialyzed against PBS, pH 7.4. Endotoxin contamination was removed by a Detoxi-Gel endotoxin removing gel step (Pierce, Rockford, IL) and probes were stored at −80°C.

To confirm AS phagocytosis in primary microglia in relation to TLR4 expression, purified microglial cell culture from wild-type and TLR4-deficient newborn mouse brains (days 1 to 3) was prepared. After removal of the meninges, cortices were minced and cells were dissociated with 0.004% DNase at 37°C and suspended in DMEM:Nutrient Mixture F-12 (DMEM/F12; Gibco Products, Invitrogen Corporation, Carlsbad, CA) supplemented with L-glutamine, 10% FCS, 100 U/mL of penicillin, and 100 μg/mL of streptomycin. Cells were plated at a density of two brains per T75 culture flask and incubated at 37°C in a humid atmosphere with 5% CO_2. Culture medium was changed twice a week. After 14 days, confluent mixed glial cultures were shaken at 180 rpm on an orbital shaker overnight at 37°C. Microglial cells in the supernatant after shaking (90% CD11b positive and 72% TLR4 positive as measured by flow cytometry, data not shown) were replated in 24-well cell culture plates at a density of 100 000 cells per well in DMEM supplemented with 10% FCS and L-glutamine. Microglial cultures were exposed to 3 μmol/L recombinant AS.

To define extracellular release of hAS from oligodendroglia overexpressing hAS under the PLP promoter, primary mixed glial culture from newborn (days 1 to 3) PLP-AS and control C57Bl/6 mice was prepared as previously described.[38] After removal of the meninges, cortices were minced and cells were dissociated with 0.004% DNase at 37°C and suspended in DMEM/F12

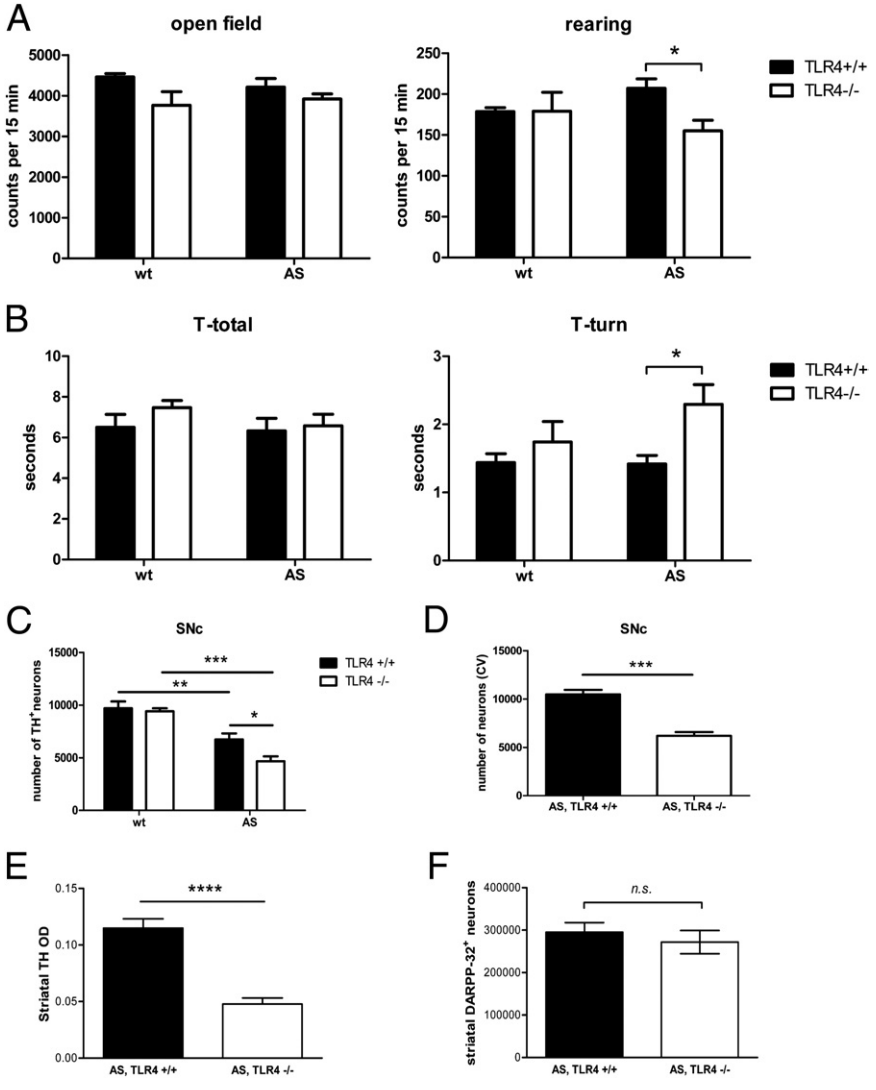

Figure 1. Locomotor deterioration and neurodegeneration in AS,TLR4$^{-/-}$ mice. **A:** Quantification of vertical (rearing) and horizontal open field activity in the Flex Field Activity System shows significant decrease of rearing behavior of AS,TLR4$^{-/-}$ mice versus AS,TLR4$^{+/+}$ mice (for each $n = 8$), whereas at baseline (wild type indicates without AS overexpression) no significant difference was detected between TLR4$^{+/+}$ mice and TLR4$^{-/-}$ mice. **B:** Pole test revealed significant increase of the time needed to turn down on a vertical pole without significant change in the total time needed to descend the pole in AS,TLR4$^{-/-}$ mice. Again at baseline (wild type indicates without AS overexpression) no significant difference was detected between TLR4$^{+/+}$ mice and TLR4$^{-/-}$ mice. Data were analyzed by two-way analysis of variance (with factors AS overexpression and TLR4 expression) with the post hoc Bonferroni test. Results are presented as mean ± SEM. **C:** Quantification of dopaminergic neurons by optical fractionator showed significantly augmented neuronal loss in SNc of AS,TLR4$^{-/-}$ mice but no nigral degeneration due to TLR4 deficiency only. Data were analyzed by two-way analysis of variance (with factors AS overexpression and TLR4 expression) with a post hoc Bonferroni test. Results are presented as mean ± SEM (for each group $n = 6$). **D:** Quantification of nigral neurons performed in cresyl violet–stained series throughout SNc confirmed amplified neuronal loss in AS,TLR4$^{-/-}$ compared with AS,TLR4$^{+/+}$ mice. **E:** Parallel to the enhanced nigral neuronal loss in AS,TLR4$^{-/-}$ mice, TH optical density (OD) measurement in striatum indicated significant loss of striatal dopaminergic fibers in AS,TLR4$^{-/-}$ mice. **F:** DARPP-32 IHC for striatal medium spiny neurons showed no significant difference between AS,TLR4$^{+/+}$ and AS,TLR4$^{-/-}$ mice. Groups were compared by unpaired two-tailed *t*-test. Results are presented as mean ± SEM (for each group $n = 6$). $^{*}P < 0.05$, $^{**}P < 0.01$, $^{***}P < 0.001$, and $^{****}P = 0.0001$.

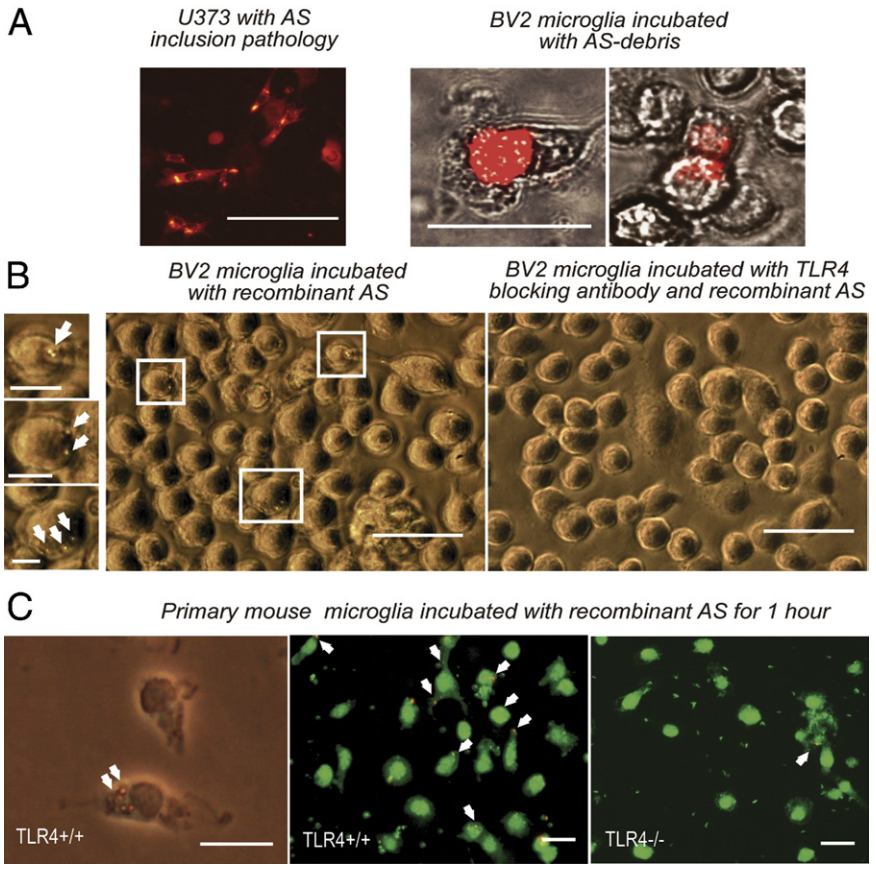

Figure 2. Phagocytosis of AS is modulated by TLR4. **A:** Genetically modified U373 cells with AS inclusion pathology as previously described[10,14,35] were killed by freeze-thaw cycle, and the resulting suspension of AS debris was used to treat BV2 immortalized microglia. After 15 minutes of incubation, large AS debris marked by red fluorescence was observed in the vicinity of microglia. After 2 hours of incubation, AS debris was almost completely incorporated by microglia and small bodies containing AS (red fluorescence) could be observed in the cytoplasm of microglial cells. Scale bar = 50 μm. **B:** Phagocytosis of recombinant AS (labeled with 15G7 antibody) by BV2 microglia was visualized by Alexa 488 green fluorescence (**arrows** point toward labeled vesicular bodies in the microglial cytoplasm). Preincubation of the BV2 cells with functional TLR4 antibody resulted in suppression of AS phagocytosis as evidenced by disappearance of the Alexa 488–labeled vesicular cytoplasmic bodies. Main scale bar = 50 μm, inset scale bar = 10 μm. **C:** Phagocytosis of recombinant AS after 1-hour incubation with primary mouse microglia ($TLR4^{+/+}$ or $TLR4^{-/-}$) was visualized with anti-hAS immunocytochemistry and Alexa 594 red fluorescence (**arrows**). Cells were counterstained with fluorescein isothiocyanate–conjugated wheat germ agglutinin (WGA), and the percentage of phagocyting cells was defined to be 40% in $TLR4^{+/+}$ microglia (123 of 300 cells analyzed) and 2% (11 of 514 cells analyzed) in $TLR4^{-/-}$ microglia. Scale bar = 10 μm.

(Gibco) supplemented with L-glutamine, 10% FCS, 100 U/mL of penicillin, and 100 μg/mL of streptomycin. Cells were plated at a density of two brains per T75 culture flask and incubated at 37°C in a humid atmosphere with 5% CO_2.

Statistical Analysis

Results are shown as the mean ± SEM, as indicated in each figure. Student's *t*-test for unpaired data or Mann-Whitney *U*-test for nonparametric data were used for sta-

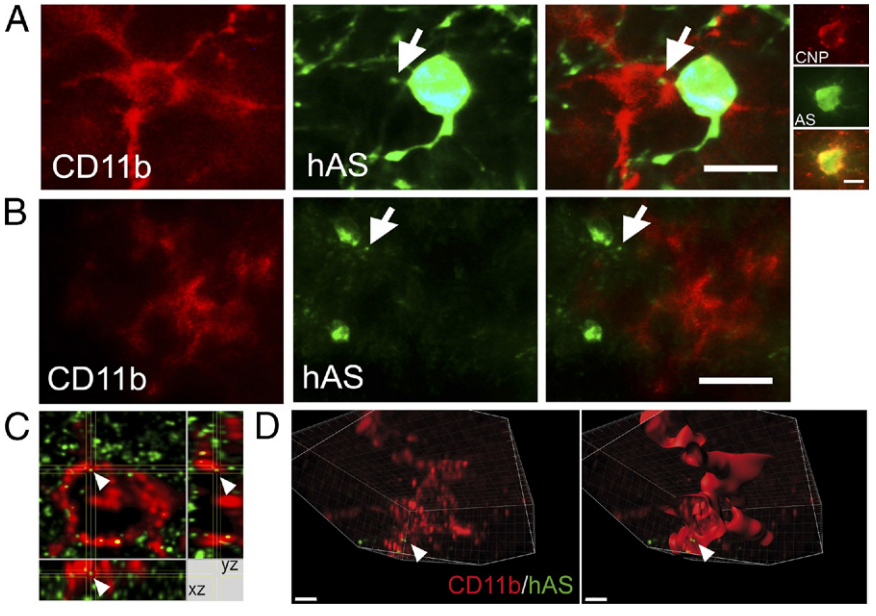

Figure 3. A: Immunofluorescence for CD11b (red) and hAS (green) in the brain of $AS,TLR4^{+/+}$ mice revealed punctuate hAS-positive structures (**arrow**) in the cytoplasm of CD11b-positive microglia opposing a hAS-expressing oligodendrocyte (scale bar = 7 μm) as evidenced by double immunofluorescence for hAS and CNP (2′,3′-cyclic nucleotide 3′-phosphohydrolase, an oligodendroglial marker, scale bar = 5 μm.). **B:** In contrast in $AS,TLR4^{-/-}$ mice hAS strictures (**arrow**) appeared only outside CD11b-positive microglia (scale bar = 15 μm). **C:** The localization of hAS in microglia of $AS,TLR4^{+/+}$ mice was further confirmed by a conventional confocal image stack showing hAS (green) dot (**arrow**) and CD11b-labeled microglia (red). Below (xz) and right (yz) views through the depth of the image stack at the position represented by the white line, demonstrating hAS-positive punctuate structure engulfed by microglia. **D:** Advanced interactive three-dimensional image analysis with isosurface reconstruction of a Z-stack of *x*-*y* sections demonstrated hAS (green, **arrow**) inside a CD11b-positive microglial cell (red). Section view in the *x*- and *y*-axes was generated by using the clipping function of Imaris x64 software. Scale bar = 2 μm.

tistical analysis, and a one-way analysis of variance was used for multiple comparisons. Two-way analysis of variance with a post hoc Bonferroni test was used when two independent factors were analyzed (eg, genotype and area or genotype and treatment as indicated in each figure). $P < 0.05$ was considered statistically significant.

Results

AS-Overexpressing Mice with Deficient TLR4 Exhibit Exacerbated Motor Disability

To evaluate the *in vivo* effects of TLR4 in a murine model of ASP, we generated AS-expressing TLR4-deficient mice (AS,TLR4$^{-/-}$) by cross-breeding AS transgenic mice expressing hAS under the control of the PLP promoter (PLP-AS mice[27]) with a mouse strain with deletion of the *TLR4* gene.[28] We analyzed the locomotion of AS,TLR4$^{-/-}$ mice compared with AS-expressing mice with normal expression of TLR4 (AS,TLR4$^{+/+}$). Motor analysis of AS,TLR4$^{+/+}$ and AS,TLR4$^{-/-}$ mice was performed at 6 months of age. Open field activity test showed impaired rearing behavior of AS,TLR4$^{-/-}$ mice versus AS,TLR4$^{+/+}$ (Figure 1A). In the pole test, the time to turn downwards on a vertical pole was increased in AS,TLR4$^{-/-}$ mice (Figure 1B). In control mice without expression of hAS, we did not detect locomotor disability induced by TLR4 deficiency alone (Figure 1).

TLR4 Deficiency in AS-Overexpressing Mice Augments Neuronal Loss in SNc and Loss of Dopaminergic Terminals in Striatum

In the control group of TLR4-deficient mice, we found a preserved number of nigral dopaminergic neurons versus control wild-type mice (Figure 1C). We have previously observed a selective susceptibility of nigral dopaminergic neurons to oligodendroglial AS overexpression in the transgenic mouse model applied here.[30] We demonstrate now that the deletion of TLR4 in the ASP model augmented dopaminergic nigral cell loss (Figure 1C) corresponding to loss of cresyl violet–stained neurons in SNc (Figure 1D) and loss of dopaminergic terminals in the striatum (Figure 1E). However, the number of striatal DARPP-32–positive GABAergic medium spiny neurons appeared unaffected by TLR4 deficiency in AS,TLR4$^{-/-}$ mice compared with AS,TLR4$^{+/+}$ mice (Figure 1F).

TLR4 Deficiency Is Associated with Disturbed Clearance of AS

Previous *in vitro* studies suggested microglia as the major scavenger cells for extracellular AS.[39] To determine whether phagocytosis of AS debris by microglia is a possible mechanism of AS clearance,[39] we first used suspension of AS debris prepared from U373 cells with hAS inclusions as previously described[10,14,35] (Figure 2A). Two hours after incubation, AS debris were incorporated in BV2 immortalized microglia (Figure 2A). Next, we found that phagocytosis of AS can be suppressed by functional blocking of TLR4 (Figure 2B). Finally, to confirm these findings, primary TLR4$^{+/+}$ and TLR4$^{-/-}$ microglia was incubated for 1 hour with recombinant AS. Forty percentage of the primary TLR4$^{+/+}$ microglia showed dotlike AS-positive profiles engulfed in the cytoplasm, whereas only 2% of primary TLR4$^{-/-}$ microglia showed phagocytosed AS in their cytoplasm (Figure 2C).

As suggested by our *in vitro* results, the accumulation of AS in the brains of AS,TLR4$^{-/-}$ mice may be due to disturbed microglial phagocytosis of AS. To confirm that hAS is secreted from transgenic oligodendroglia into the extracellular space, we measured by ELISA the release of hAS in the supernatant of mixed glial cultures prepared from PLP-AS mice and detected levels of 1.24 to 5.24 ng/mL of hAS. Next, *in vivo* phagocytosis of hAS by microglia was shown in brains of AS,TLR4$^{+/+}$ mice (Figure 3A); however, it was not readily detectable in AS,TLR4$^{-/-}$ mice (Figure 3B). This finding was confirmed by confocal microscopy and three-dimensional analysis of confocal images with Imaris x64 software and isosurface recon-

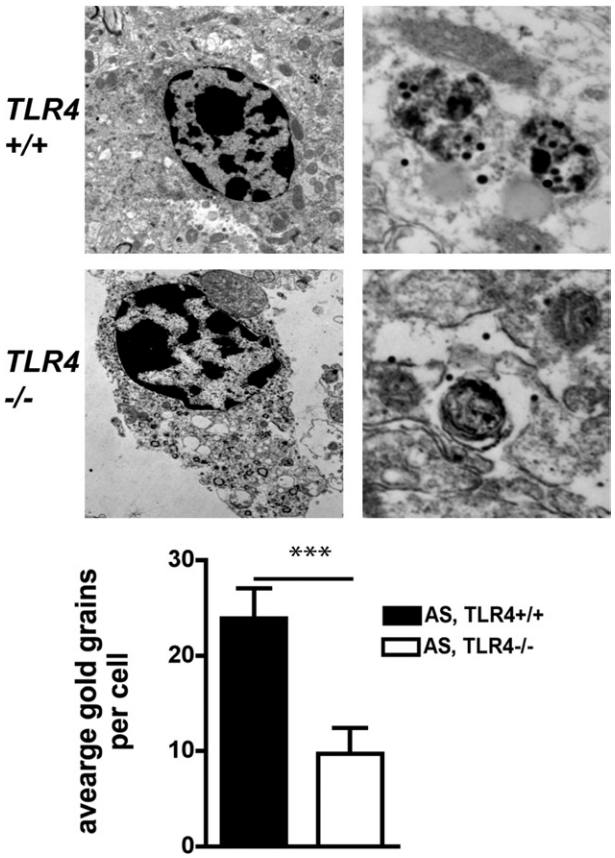

Figure 4. Electron microscopic analysis of the brains of AS,TLR4$^{+/+}$ and AS,TLR4$^{-/-}$ mice. Microglia and macrophage cells were identified close to the perivascular areas by their elongated nucleus with condensed chromatin and abundant lysosomes and phagocytic organelles in the cytoplasm. In AS,TLR4$^{+/+}$ mice, microglia and macrophages showed abundant gold particles in association with phagosomes and lysosomes. In contrast, microglia and macrophages of AS,TLR4$^{-/-}$ mice had fewer gold particles in phagocytic cytoplasmic organelles as defined by the number of gold grains per microglia and macrophage cell ($n = 125$ for each). Original magnification, ×5000 and ×25,000, respectively. ***$P = 0.001$.

Figure 5. Effect of TLR4 ablation on AS brain levels. Four animals per group were used to dissect the forebrain and midbrain and prepare lysates for measurement of hAS protein concentration by ELISA. Two-way analysis of variance (with factors genotype and area) with a post hoc Bonferroni test showed a significant increase of hAS protein concentration in both the forebrain and midbrain of AS,TLR4$^{-/-}$ mice. ***$P = 0.001$, ****$P < 0.0001$.

struction of AS-positive vesicular bodies within CD11b-positive microglia (Figure 3C).

Ultrastructural analysis was further used to determine the phagocytic activity of microglia in AS,TLR4$^{+/+}$ and AS,TLR4$^{-/-}$ mice. Microglia and macrophage cells were identified by their morphologic characteristics and close proximity to perivascular areas. These cells usually have an elongated nucleus with condensed chromatin and contain abundant lysosomes and phagocytic organelles. Immunogold labeling for AS in AS,TLR4$^{+/+}$ and AS,TLR4$^{-/-}$ mice was localized in oligodendroglial cells in association with the inner and outer mitochondrial membranes and cytoplasmic structures (data not shown). In the AS,TLR4$^{+/+}$ mice abundant gold particles were found in association with phagosomes and lysosomes in microglia, whereas in AS,TLR4$^{-/-}$ mice there were fewer gold particles in phagocytic cytoplasmic organelles (Figure 4).

Finally, to analyze the effect of TLR4 deficiency on AS level in transgenic mice *in vivo*, hAS concentration in the midbrain and forebrain was measured by ELISA and showed a significant increase in AS,TLR4$^{-/-}$ mice compared with AS,TLR4$^{+/+}$ mice (Figure 5).

AS,TLR4$^{-/-}$ Mice Present with Increased Levels of TNF-α in the Midbrain Associated with Proinflammatory Astroglial Response

Analysis of brain concentrations of several inflammatory modulators was performed by fluorometric multiplex bead–based cytokine immunoassay. An unexpected region-specific increase of TNF-α concentration in the midbrain was detected in AS,TLR4$^{-/-}$ mice (Figure 6A). However, other cytokines, including IL-6, IFN-γ, GM-CSF, IL-10, and IL-1α, did not show significant differences between AS,TLR4$^{-/-}$ and AS,TLR4$^{+/+}$ mice in either the midbrain or forebrain (Figure 6A). To define the cell source of TNF-α in the midbrain of AS,TLR4$^{-/-}$ mice, double immunofluorescence labeling was performed. Predominant colocalization of GFAP and TNF-α was evidenced in the SNc of AS,TLR4$^{-/-}$ mice (Figure 6B).

Discussion

Up-regulation of TLRs has been demonstrated in brains with ASPs, such as PD, DLB, and MSA, highlighting innate immunity as a novel therapeutic target in these disorders.[15,16] We show that TLR4 is an important mediator of microglial phagocytosis of AS. We demonstrate deleterious effects of TLR4 ablation in a transgenic mouse model of MSA.[15,40–42] Motor impairment and loss of nigrostriatal dopaminergic neurons and fibers were significantly aggravated in TLR4-deficient mice with hAS overexpression. This phenotype was associated with increased AS accumulation throughout the brain, implicating TLR4 signaling in the pathogenesis of ASPs. We propose that TLR4 up-regulation in microglia is a natural mechanism to boost the clearance of extracellular AS in ASPs. Similar to previous studies that demonstrated AS secretion from neuronal cells,[43,44] we show that oligodendroglial cells overexpressing hAS are also able to secrete

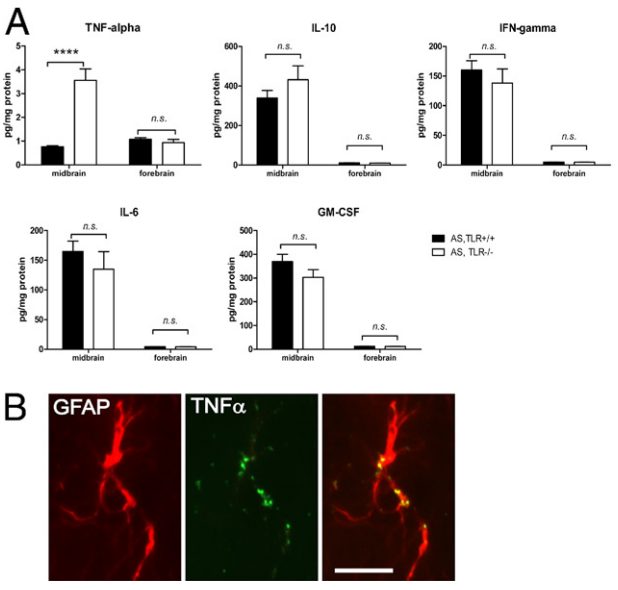

Figure 6. Inflammatory mediation in ASPs in the absence of TLR4. **A:** Flow cytomix analysis of IL-10, IFN-γ, IL-6, and GM-CSF in midbrain and forebrain lysates demonstrated no significant differences between AS,TLR4$^{+/+}$ and AS,TLR4$^{-/-}$ mice. However, strongly increased production of TNF-α was detected in the midbrain of AS,TLR4$^{-/-}$ mice. For all analyses, $n = 6$ (excluding IL-10 AS,TLR4$^{-/-}$ mice, $n = 4$). Data were analyzed by two-way analysis of variance (with factors genotype and area) with a post hoc Bonferroni test. Results are presented as mean ± SEM. **B:** Immunofluorescence in SNc of AS,TLR4$^{-/-}$ mice identified GFAP-positive astroglia (red) as the main source of TNF-α (green). Scale bar = 10 μm. ****$P < 0.0001$.

the protein extracellularly, where it becomes available to microglia. Liu et al[45] previously described endocytosis of fibrillar AS by microglia. The scavenger role of microglia for extracellular AS has been proposed also by Lee et al.[39] We expand these findings by *in vitro* observations of cytoplasmic AS incorporation in microglial cells *in vitro*. Further, microglial phagocytosis of extracellular AS was demonstrated in PLP-AS mice by immunofluorescent AS-positive dotlike cytoplasmic deposits or AS-immunogold labeling within microglial phagosomes. Functional blocking or knock down of TLR4 in microglia resulted in suppression of AS phagocytosis *in vitro,* and TLR4 ablation *in vivo* led to reduced phagocytosis by microglia associated with accumulation of AS in the mouse brain. These results confirm the role of TLR4-mediated clearance of extracellular AS by microglia, the main cell type bearing TLR4 in the brain; however, the exact mechanisms need further elucidation. In summary, impaired TLR4-regulated AS clearance appears to exacerbate neurodegeneration by increasing AS accumulation, which is especially toxic to nigral dopaminergic neurons,[5,46] therefore contributing to the pathogenesis of ASPs.

Parallel to the increased accumulation of AS that may directly exert toxicity, we identified enhanced proinflammatory signaling with increased production of TNF-α in the midbrain of AS,TLR4$^{-/-}$ mice. Double staining enabled us to define astroglia as the main source of TNF-α in SNc of AS,TLR4$^{-/-}$ mice. The exact mechanism of this proinflammatory response will need further elucidation. A possible pathway may be the direct transfer of AS leading to an enhanced proinflammatory response by astroglia as recently suggested.[47] The selectively increased proinflammatory response in the midbrain of AS,TLR4$^{-/-}$ mice *in vivo* may be related to the increased oxidative stress milieu in SNc, associated with augmented cell death of nigral dopaminergic neurons under the exposure to higher concentrations of AS.[48,49] The increased levels of TNF-α may further trigger the direct cell death of dopaminergic neurons.[50] Altogether these events contribute to the vicious circle of progressive neurodegeneration in SNc in AS,TLR4$^{-/-}$ mice.

The finding of enhanced nigral neuropathologic characteristics in AS,TLR4$^{-/-}$ mice is supported by our behavioral observations. The locomotor phenotype of mice in the present study was analyzed applying two nigrostriatal pathway–dependent tests. The pole test is used to assess basal ganglia–related movement disorders in mice[29,51–56] and involves several aspects of motor function, including movement initiation, balance, coordination, and bradykinesia, due to a hypodopaminergic state rather than cerebellar abnormalities. Changes in rearing behavior provide an early sign of basal ganglia dysfunction reflected in disturbed locomotor activity[57] and strengthen the finding that the motor phenotype observed in AS,TLR4$^{-/-}$ mice corresponds to the underlying striatonigral pathologic features consistent with previous reports on mouse models of PD.[55,56,58]

We demonstrate now by *in vitro* and *in vivo* methods that TLR4 is involved in the process of extracellular AS uptake and clearance. On the basis of our current work, we propose that TLR4 signaling participates in an endogenous neuroprotective mechanism in ASPs, similar to other protein-misfolding disorders. Recently, Spinner et al[59] reported increased disease-specific prion protein PrP^{Sc} accumulation and reduced immune recognition and response to PrP^{Sc} in TLR4-deficient mice compared with wild-type animals, consistent with our current observations in a model of ASPs with TLR4 ablation. Furthermore, a similar mechanism involving TLRs appears to be operative in the clearance of amyloid-β in Alzheimer's disease—another neurodegenerative disorder with a prionlike pathogenesis.[21–24,60]

How plausible is it to target TLR4 responses in ASPs to modify disease progression? Although administration of TLR4 ligands may activate phagocytosis and clearance of AS deposits and be related to beneficial effects, TLR4 agonist treatment could lead also to dangerous adverse effects associated with the induction of high levels of proinflammatory mediators.[61–63] The proinflammatory signaling induced by TLR4 agonists may be counteracted by co-application of specific antagonists to neutralize the involved proinflammatory cytokines but enhance the phagocytic activity related to improved clearance of the toxic protein species. This approach will necessitate further preclinical investigations to define its feasibility in ASPs.

In summary, in this study we show that misbalanced TLR4 signaling may play a crucial role in ASP progression. The TLR4-dependent pathway represents an important AS clearance mechanism. The present data emphasize the importance of functional clearance mechanisms related to a "healthy" microglial response in ASPs and support the hypothesis that progression of PD and related disorders with AS pathologic characteristics may result from a primary long-term impairment of microglia, reflecting age-related dysfunction or genetic predisposition. The current findings have significant implications for the development of novel disease-modifying therapies for ASPs.

Acknowledgments

We are grateful to Monika Hainzer for her excellent technical assistance in genotyping, IHC, and ELISA. Confocal microscopy was performed at the Biooptics Core Facility of Innsbruck Medical University, Innsbruck, Austria.

References

1. Gasser T: Molecular pathogenesis of Parkinson disease: insights from genetic studies. Expert Rev Mol Med 2009, 11:e22
2. Scholz SW, Houlden H, Schulte C, Sharma M, Li A, Berg D, et al: SNCA variants are associated with increased risk for multiple system atrophy. Ann Neurol 2009, 65:610–614
3. Al-Chalabi A, Durr A, Wood NW, Parkinson MH, Camuzat A, Hulot JS, Morrison KE, Renton A, Sussmuth SD, Landwehrmeyer BG, Ludolph A, Agid Y, Brice A, Leigh PN, Bensimon G: Genetic variants of the alpha-synuclein gene SNCA are associated with multiple system atrophy. PLoS One 2009, 4:e7114
4. Danzer KM, Ruf WP, Putcha P, Joyner D, Hashimoto T, Glabe C, Hyman BT, McLean PJ: Heat-shock protein 70 modulates toxic extracellular α-synuclein oligomers and rescues trans-synaptic toxicity. FASEB J 2010, 25:326–336
5. Cookson MR: α-Synuclein and neuronal cell death. Mol Neurodegener 2009, 4:9

6. Xilouri M, Vogiatzi T, Vekrellis K, Park D, Stefanis L: Abberant alpha-synuclein confers toxicity to neurons in part through inhibition of chaperone-mediated autophagy. PLoS One 2009, 4:e5515
7. Lee HJ, Khoshaghideh F, Lee S, Lee SJ: Impairment of microtubule-dependent trafficking by overexpression of alpha-synuclein. Eur J Neurosci 2006, 24:3153–3162
8. Cooper AA, Gitler AD, Cashikar A, Haynes CM, Hill KJ, Bhullar B, Liu K, Xu K, Strathearn KE, Liu F, Cao S, Caldwell KA, Caldwell GA, Marsischky G, Kolodner RD, Labaer J, Rochet JC, Bonini NM, Lindquist S: Alpha-Synuclein blocks ER-Golgi traffic and Rab1 rescues neuron loss in Parkinson's models. Science 2006, 313:324–328
9. Chen Q, Thorpe J, Keller JN: Alpha-synuclein alters proteasome function, protein synthesis, and stationary phase viability. J Biol Chem 2005, 280:30009–30017
10. Stefanova N, Schanda K, Klimaschewski L, Poewe W, Wenning GK, Reindl M: Tumor necrosis factor-alpha-induced cell death in U373 cells overexpressing alpha-synuclein. J Neurosci Res 2003, 73:334–340
11. Shults CW, Rockenstein E, Crews L, Adame A, Mante M, Larrea G, Hashimoto M, Song D, Iwatsubo T, Tsuboi K, Masliah E: Neurological and neurodegenerative alterations in a transgenic mouse model expressing human alpha-synuclein under oligodendrocyte promoter: implications for multiple system atrophy. J Neurosci 2005, 25:10689–10699
12. Lashuel HA, Petre BM, Wall J, Simon M, Nowak RJ, Walz T, Lansbury PT Jr: Alpha-synuclein, especially the Parkinson's disease-associated mutants, forms pore-like annular and tubular protofibrils. J Mol Biol 2002, 322:1089–1102
13. Stefanis L, Larsen KE, Rideout HJ, Sulzer D, Greene LA: Expression of A53T mutant but not wild-type alpha-synuclein in PC12 cells induces alterations of the ubiquitin-dependent degradation system, loss of dopamine release, and autophagic cell death. J Neurosci 2001, 21:9549–9560
14. Stefanova N, Klimaschewski L, Poewe W, Wenning GK, Reindl M: Glial cell death induced by overexpression of alpha-synuclein. J Neurosci Res 2001, 65:432–438
15. Stefanova N, Reindl M, Neumann M, Kahle PJ, Poewe W, Wenning GK: Microglial activation mediates neurodegeneration related to oligodendroglial alpha-synucleinopathy: implications for multiple system atrophy. Mov Disord 2007, 22:2196–2203
16. Letiembre M, Liu Y, Walter S, Hao W, Pfander T, Wrede A, Schulz-Schaeffer W, Fassbender K: Screening of innate immune receptors in neurodegenerative diseases: a similar pattern. Neurobiol Aging 2009, 30:759–768
17. Glezer I, Simard AR, Rivest S: Neuroprotective role of the innate immune system by microglia. Neuroscience 2007, 147:867–883
18. Medzhitov R: Toll-like receptors and innate immunity. Nat Rev Immunol 2001, 1:135–145
19. Caso JR, Pradillo JM, Hurtado O, Lorenzo P, Moro MA, Lizasoain I: Toll-like receptor 4 is involved in brain damage and inflammation after experimental stroke. Circulation 2007, 115:1599–1608
20. Caso JR, Pradillo JM, Hurtado O, Leza JC, Moro MA, Lizasoain I: Toll-like receptor 4 is involved in subacute stress-induced neuroinflammation and in the worsening of experimental stroke. Stroke 2008, 39:1314–1320
21. Liu Y, Walter S, Stagi M, Cherny D, Letiembre M, Schulz-Schaeffer W, Heine H, Penke B, Neumann H, Fassbender K: LPS receptor (CD14): a receptor for phagocytosis of Alzheimer's amyloid peptide. Brain 2005, 128:1778–1789
22. Tahara K, Kim HD, Jin JJ, Maxwell JA, Li L, Fukuchi K: Role of toll-like receptor signalling in Abeta uptake and clearance. Brain 2006, 129:3006–3019
23. Chen K, Iribarren P, Hu J, Chen J, Gong W, Cho EH, Lockett S, Dunlop NM, Wang JM: Activation of Toll-like receptor 2 on microglia promotes cell uptake of Alzheimer disease-associated amyloid beta peptide. J Biol Chem 2006, 281:3651–3659
24. Richard KL, Filali M, Prefontaine P, Rivest S: Toll-like receptor 2 acts as a natural innate immune receptor to clear amyloid beta 1–42 and delay the cognitive decline in a mouse model of Alzheimer's disease. J Neurosci 2008, 28:5784–5793
25. Magen I, Chesselet MF: Genetic mouse models of Parkinson's disease: the state of the art. Prog Brain Res 2010, 184:53–87
26. Stefanova N, Tison F, Reindl M, Poewe W, Wenning GK: Animal models of multiple system atrophy. Trends Neurosci 2005, 28:501–506
27. Kahle PJ, Neumann M, Ozmen L, Muller V, Jacobsen H, Spooren W, Fuss B, Mallon B, Macklin WB, Fujiwara H, Hasegawa M, Iwatsubo T, Kretzschmar HA, Haass C: Hyperphosphorylation and insolubility of alpha-synuclein in transgenic mouse oligodendrocytes. EMBO Rep 2002, 3:583–588
28. Poltorak A, He X, Smirnova I, Liu MY, Van Huffel C, Du X, Birdwell D, Alejos E, Silva M, Galanos C, Freudenberg M, Ricciardi-Castagnoli P, Layton B, Beutler B: Defective LPS signaling in C3H/HeJ and C57BL/10ScCr mice: mutations in Tlr4 gene. Science 1998, 282:2085–2088
29. Fernagut PO, Diguet E, Stefanova N, Biran M, Wenning GK, Canioni P, Bioulac B, Tison F: Subacute systemic 3-nitropropionic acid intoxication induces a distinct motor disorder in adult C57B1/6 mice: behavioural and histopathological characterisation. Neuroscience 2002, 114:1005–1017
30. Stefanova N, Reindl M, Neumann M, Haass C, Poewe W, Kahle PJ, Wenning GK: Oxidative stress in transgenic mice with oligodendroglial alpha-synuclein overexpression replicates the characteristic neuropathology of multiple system atrophy. Am J Pathol 2005, 166:869–876
31. Stefanova N, Poewe W, Wenning GK: Rasagiline is neuroprotective in a transgenic model of multiple system atrophy. Exp Neurol 2008, 210:421–427
32. Wu DC, Jackson-Lewis V, Vila M, Tieu K, Teismann P, Vadseth C, Choi DK, Ischiropoulos H, Przedborski S: Blockade of microglial activation is neuroprotective in the 1-methyl-4-phenyl-1,2,3,6-tetrahydropyridine mouse model of Parkinson disease. J Neurosci 2002, 22:1763–1771
33. Marongiu R, Spencer B, Crews L, Adame A, Patrick C, Trejo M, Dallapiccola B, Valente EM, Masliah E: Mutant Pink1 induces mitochondrial dysfunction in a neuronal cell model of Parkinson's disease by disturbing calcium flux. J Neurochem 2009, 108:1561–1574
34. Rockenstein E, Mallory M, Mante M, Sisk A, Masliaha E: Early formation of mature amyloid-beta protein deposits in a mutant APP transgenic model depends on levels of Abeta(1–42). J Neurosci Res 2001, 66:573–582
35. Stefanova N, Emgard M, Klimaschewski L, Wenning GK, Reindl M: Ultrastructure of alpha-synuclein-positive aggregations in U373 astrocytoma and rat primary glial cells. Neurosci Lett 2002, 323:37–40
36. Gan L, Ye S, Chu A, Anton K, Yi S, Vincent VA, von SD, Chin D, Murray J, Lohr S, Patthy L, Gonzalez-Zulueta M, Nikolich K, Urfer R: Identification of cathepsin B as a mediator of neuronal death induced by Abeta-activated microglial cells using a functional genomics approach. J Biol Chem 2004, 279:5565–5572
37. Blasi E, Barluzzi R, Bocchini V, Mazzolla R, Bistoni F: Immortalization of murine microglial cells by a v-raf/v-myc carrying retrovirus. J Neuroimmunol 1990, 27:229–237
38. Lotz M, Ebert S, Esselmann H, Iliev AI, Prinz M, Wiazewicz N, Wiltfang J, Gerber J, Nau R: Amyloid beta peptide 1–40 enhances the action of Toll-like receptor-2 and -4 agonists but antagonizes Toll-like receptor-9-induced inflammation in primary mouse microglial cell cultures. J Neurochem 2005, 94:289–298
39. Lee HJ, Suk JE, Bae EJ, Lee SJ: Clearance and deposition of extracellular alpha-synuclein aggregates in microglia. Biochem Biophys Res Commun 2008, 372:423–428
40. Chung YC, Kim SR, Jin BK: Paroxetine prevents loss of nigrostriatal dopaminergic neurons by inhibiting brain inflammation and oxidative stress in an experimental model of Parkinson's disease. J Immunol 2010, 185:1230–1237
41. Cho Y, Son HJ, Kim EM, Choi JH, Kim ST, Ji IJ, Choi DH, Joh TH, Kim YS, Hwang O: Doxycycline is neuroprotective against nigral dopaminergic degeneration by a dual mechanism involving MMP-3. Neurotox Res 2009, 16:361–371
42. Hirsch EC, Hunot S: Neuroinflammation in Parkinson's disease: a target for neuroprotection? Lancet Neurol 2009, 8:382–397
43. Lee HJ, Patel S, Lee SJ: Intravesicular localization and exocytosis of alpha-synuclein and its aggregates. J Neurosci 2005, 25:6016–6024
44. Desplats P, Lee HJ, Bae EJ, Patrick C, Rockenstein E, Crews L, Spencer B, Masliah E, Lee SJ: Inclusion formation and neuronal cell death through neuron-to-neuron transmission of alpha-synuclein. Proc Natl Acad Sci U S A 2009, 106:13010–13015
45. Liu J, Zhou Y, Wang Y, Fong H, Murray TM, Zhang J: Identification of proteins involved in microglial endocytosis of alpha-synuclein. J Proteome Res 2007, 6:3614–3627

46. Zhang W, Wang T, Pei Z, Miller DS, Wu X, Block ML, Wilson B, Zhang W, Zhou Y, Hong JS, Zhang J: Aggregated alpha-synuclein activates microglia: a process leading to disease progression in Parkinson's disease. FASEB J 2005, 19:533–542
47. Lee HJ, Suk JE, Patrick C, Bae EJ, Cho JH, Rho S, Hwang D, Masliah E, Lee SJ: Direct transfer of alpha-synuclein from neuron to astroglia causes inflammatory responses in synucleinopathies. J Biol Chem 2010, 285:9262–9272
48. Jenner P: Oxidative stress in Parkinson's disease. Ann Neurol 2003, 53(Suppl 3):S26–S36
49. Moore DJ, West AB, Dawson VL, Dawson TM: Molecular pathophysiology of Parkinson's disease. Annu Rev Neurosci 2005, 28:57–87
50. De Lella Ezcurra AL, Chertoff M, Ferrari C, Graciarena M, Pitossi F: Chronic expression of low levels of tumor necrosis factor-alpha in the substantia nigra elicits progressive neurodegeneration, delayed motor symptoms and microglia/macrophage activation. Neurobiol Dis 2010, 37:630–640
51. Ogawa N, Hirose Y, Ohara S, Ono T, Watanabe Y: A simple quantitative bradykinesia test in MPTP-treated mice. Res Commun Chem Pathol Pharmacol 1985, 50:435–441
52. Ogawa N, Mizukawa K, Hirose Y, Kajita S, Ohara S, Watanabe Y: MPTP-induced parkinsonian model in mice: biochemistry, pharmacology and behavior. Eur Neurol 1987, 26(Suppl 1):16–23
53. Matsuura K, Kabuto H, Makino H, Ogawa N: Pole test is a useful method for evaluating the mouse movement disorder caused by striatal dopamine depletion. J Neurosci Methods 1997, 73:45–48
54. Sedelis M, Hofele K, Auburger GW, Morgan S, Huston JP, Schwarting RK: MPTP susceptibility in the mouse: behavioral, neurochemical, and histological analysis of gender and strain differences. Behav Genet 2000, 30:171–182
55. Fleming SM, Salcedo J, Fernagut PO, Rockenstein E, Masliah E, Levine MS, Chesselet MF: Early and progressive sensorimotor anomalies in mice overexpressing wild-type human alpha-synuclein. J Neurosci 2004, 24:9434–9440
56. Rommelfanger KS, Edwards GL, Freeman KG, Liles LC, Miller GW, Weinshenker D: Norepinephrine loss produces more profound motor deficits than MPTP treatment in mice. Proc Natl Acad Sci U S A 2007, 104:13804–13809
57. Fleming SM, Zhu C, Fernagut PO, Mehta A, DiCarlo CD, Seaman RL, Chesselet MF: Behavioral and immunohistochemical effects of chronic intravenous and subcutaneous infusions of varying doses of rotenone. Exp Neurol 2004, 187:418–429
58. Hwang DY, Fleming SM, Ardayfio P, Moran-Gates T, Kim H, Tarazi FI, Chesselet MF, Kim KS: 3,4-dihydroxyphenylalanine reverses the motor deficits in Pitx3-deficient aphakia mice: behavioral characterization of a novel genetic model of Parkinson's disease. J Neurosci 2005, 25:2132–2137
59. Spinner DS, Cho IS, Park SY, Kim JI, Meeker HC, Ye X, Lafauci G, Kerr DJ, Flory MJ, Kim BS, Kascsak RB, Wisniewski T, Levis WR, Schuller-Levis GB, Carp RI, Park E, Kascsak RJ: Accelerated prion disease pathogenesis in Toll-like receptor 4 signaling-mutant mice. J Virol 2008, 82:10701–10708
60. Frost B, Diamond MI: Prion-like mechanisms in neurodegenerative diseases. Nat Rev Neurosci 2010, 11:155–159
61. Combrinck MI, Perry VH, Cunningham C: Peripheral infection evokes exaggerated sickness behaviour in pre-clinical murine prion disease. Neuroscience 2002, 112:7–11
62. Cunningham C, Wilcockson DC, Campion S, Lunnon K, Perry VH: Central and systemic endotoxin challenges exacerbate the local inflammatory response and increase neuronal death during chronic neurodegeneration. J Neurosci 2005, 25:9275–9284
63. Ohta S, Bahrun U, Shimazu R, Matsushita H, Fukudome K, Kimoto M: Induction of long-term lipopolysaccharide tolerance by an agonistic monoclonal antibody to the toll-like receptor 4/MD-2 complex. Clin Vaccine Immunol 2006, 13:1131–1136